Fabrication of X-Ray Microcalorimeter Focal Planes Composed of Two Distinct Pixel Types

Edward J. Wassell, Joseph S. Adams, Simon R. Bandler, Gabriele L. Betancourt-Martinez, Meng P. Chiao, Meng Ping Chang, James A. Chervenak, Aaron M. Datesman, Megan E. Eckart, Audrey J. Ewin, Fred Michael Finkbeiner, Jong Yoon Ha, Richard Kelley, Caroline A. Kilbourne, Antoine R. Miniussi, Kazuhiro Sakai, Frederick Scott Porter, John E. Sadleir, Stephen James Smith, Nicholas A. Wakeham, and Wonisk Yoon

***Abstract*—We develop superconducting transition-edge sensor (TES) microcalorimeter focal planes for versatility in meeting the specifications of X-ray imaging spectrometers, including high count rate, high energy resolution, and large field of view. In particular, a focal plane composed of two subarrays: one of fine pitch, high count-rate devices and the other of slower, larger pixels with similar energy resolution, offers promise for the next generation of astrophysics instruments, such as the X-ray Integral Field Unit Instrument on the European Space Agency's ATHENA mission. We have based the subarrays of our current design on successful pixel designs that have been demonstrated separately. Pixels with an all-gold X-ray absorber on 50 and 75 μm pitch, where the Mo/Au TES sits atop a thick metal heatsinking layer, have shown high resolution and can accommodate high count rates. The demonstrated larger pixels use a silicon nitride membrane for thermal isolation, thinner Au, and an added bismuth layer in a 250-μm^2 absorber. To tune the parameters of each subarray requires merging the fabrication processes of the two detector types. We present the fabrication process for dual production of different X-ray absorbers on the same substrate, thick Au on the small pixels and thinner Au with a Bi capping layer on the larger pixels to tune their heat capacities. The process requires multiple electroplating and etching steps, but the absorbers are defined in a single-ion milling step. We demonstrate methods for integrating the heatsinking of the two types of pixel into the same focal plane consistent with the requirements for each subarray, including the limiting of thermal crosstalk. We also discuss fabrication process modifications for tuning the intrinsic transition temperature (T_c) of the bilayers for the different device types through variation of the bilayer thicknesses. The latest results on these "hybrid" arrays will be presented.**

***Index Terms*—Arrays, low temperature detectors, microcalorimeters, transition-edge sensors (TES), X-ray spectroscopy.**

Manuscript received September 6, 2016; accepted November 22, 2016. Date of publication December 1, 2016; date of current version December 30, 2016. This work was supported by NASA (Office of Space Science, Contract NNX11AB47G from ROSES 2009).

E. J. Wassell and A. M. Datesman are with the NASA Goddard Space Flight Center, Greenbelt, MD 20771 USA, and also with the Stinger-Ghaffarian Technologies, Inc., Greenbelt, MD 20771 USA (e-mail: edward.wassell@nasa.gov; aaron.m.datesman@nasa.gov).

J. S. Adams and S. J. Smith are with the NASA Goddard Space Flight Center, Greenbelt, MD 20771 USA, and also with CRESST, University of Maryland, College Park, MD 20742 USA (e-mail: Joseph.S.Adams@nasa.gov; stephen.j.smith@nasa.gov).

S. R. Bandler, M. P. Chiao, M. P. Chang, J. A. Chervenak, M. E. Eckart, A. J. Ewin, R. Kelley, C. A. Kilbourne, A. R. Miniussi, F. S. Porter, and J. E. Sadleir are with the NASA Goddard Space Flight Center, Greenbelt, MD 20771 USA (e-mail: Simon.R.Bandler@nasa.gov; meng.p.chiao@nasa.gov; meng-ping.chang@nasa.gov; James.A.Chervenak@nasa.gov; Megan.E.Eckart@nasa.gov; Audrey.J.Ewin@nasa.gov; Richard.L.Kelley@nasa.gov; Caroline.A.Kilbourne@nasa.gov; antoine.r.miniussi@nasa.gov; Frederick.S.Porter@nasa.gov; john.e.sadleir@nasa.gov).

G. L. Betancourt-Martinez is with the NASA Goddard Space Flight Center, Greenbelt, MD 20771 USA, and also with the University of Maryland, College Park, MD 20742 USA (e-mail: Gabriele.L.Betancourt-Martinez@nasa.gov).

F. M. Finkbeiner is with the NASA Goddard Space Flight Center, Greenbelt, MD 20771 USA, and also with the Wyle Information Systems, McLean, VA 22102 USA (e-mail: Fred.M.Finkbeiner@nasa.gov).

J. Y. Ha is with the NASA Goddard Space Flight Center, Greenbelt, MD 20771 USA, and also with the SB Microsystems, Inc., Glen Burnie, MD 20161 USA (e-mail: jongyoon.ha@sbmicrosystems.us).

K. Sakai, N. A. Wakeham, and W. Yoon are with the NASA Goddard Space Flight Center, Greenbelt, MD 20771 USA, and also with the Universities Space Research Association, Columbia, MD 21046 USA (e-mail: kazuhiro.sakai@nasa.gov; Nicholas.a.wakeham@nasa.gov; wonsik.yoon@nasa.gov).

Color versions of one or more of the figures in this paper are available online at http://ieeexplore.ieee.org.

Digital Object Identifier 10.1109/TASC.2016.2633783

I. Introduction

THE Advanced Telescope for High ENergy Astrophysics (ATHENA) X-ray Observatory was selected in 2014 to study the hot and energetic universe [1]. One of two instruments proposed to be interchanged at the focal plane is the X-ray Integral Field Unit (X-IFU), a cryogenic microcalorimeter array with a 5' field-of-view comprised of superconducting thin film transition-edge sensors (TES) biased along the slope of the superconducting to normal resistive transition.

Presently there are two different detector array concepts under consideration for the focal plane of X-IFU aimed at achieving the demanding goal of observing sources with a 10 mCrab count rate while maintaining 2.5 eV energy resolution [2], [3]. One concept is a uniform array of 3840 large pixels on a 249 μm pitch which would achieve the high count-rate goal by an optical defocusing of the point spread function over a large fraction of the array. The other concept with which this paper is concerned achieves this goal through the fabrication of a hybrid array incorporating two distinct pixel types, a small pixel array (SPA) consisting of 324 fast pixels of 110 μm pitch in the same focal plane as a large pixel array (LPA) of slower 260 μm pixel pitch.

This paper reports upon three technology developments required to successfully yield hybrid arrays of two different pixel types. First, we demonstrate the fabrication of a single array of pixels with two superconducting transition temperatures (T_c). Next, we show how to fabricate pixels with two distinct absorber

types to separately tune their respective heat capacities (C_v). Then, we describe how we separately tune the thermal conductance (G_b) to the bath by the addition of copper to the backside of the silicon nitride membranes which support the detectors. Finally, we report on our first attempt to incorporate all three technologies in a single array.

II. Fabrication of Pixels With Two Distinct $T_{\rm ci}$

Engineering control of T_c in the superconducting bilayer TES is important for optimizing the performance of the two pixel types. The total heat capacity and the thermal decay time are both functions of the operating transition temperature T_0, the apparent transition temperature when the device is voltage biased into its superconducting transition. As the size of the pixel is reduced, the longitudinal proximity effect from the superconducting Nb leads affects the superconducting state of the detector significantly, such that T_c can differ from $T_{\rm ci}$, the intrinsic transition temperature of the Mo/Au bilayer in isolation. [4] The addition of normal metal noise reducing features to the TES has been shown both to lower T_c and change the shape of the transition, and these added features have a greater effect as the size of the TES is reduced [5]. Conversely, on account of the longitudinal proximity effect, reducing the size of the TES and consequently lead separation enhances the superconducting order parameter in the TES film and effectively raises T_c [4]. Further, applying a voltage bias to hold the TES in its superconducting transition affects the operational T_0.

For pixel designs selected for devices in our two pixel type array, the small pixel which has a 35 $\times$ 35 micron bilayer region shows T_0 differing from $T_{\rm ci}$ by 45 mK, whereas in a large pixel ($>$100 μm) the difference between T_0 and $T_{\rm ci}$ is usually less than $<$5 mK [3], [6], [7]. By engineering distinct $T_{\rm ci}$ for each of the two pixel regions, we gain flexibility in tuning each array separately to meet different count-rate and energy resolution specifications.

The Mo/Au bilayers in this study consist of magnetron sputtered Mo with a sputtered Au capping layer to prevent oxidation of the superconducting Mo film. Following a brief in situ ion mill clean, thick Au is added to tune to the target $T_{\rm ci}(1)$ of the SPA via electron beam deposition. Protective photoresist is added to the $T_{\rm ci}(1)$ regions of the wafer and the exposed Au is ion milled to create the LPA $T_{\rm ci}(2)$ region. Then we photolithographically define the TES and ion mill the Au from the rest of the wafer leaving a thin layer of Moly to be removed later except for a small step to provide a contact region between the TES and the Nb leads. Since the etch rate selectivity of gold to molybdenum in the ion mill is 3:1, our process permits a differential thickness of the Au of about 75 nm corresponding to an additional 25 nm overetch into the thin Mo layer of the bilayer as we ion mill the Au film to define the TES.

A demonstration of this technique was undertaken in which we removed 50 nm Au from the SPA region and found a 30 mK difference in $T_{\rm ci}$. If we removed 75 nm of Au as our process permits, we should be able to yield a hybrid array with a $\Delta T_{\rm ci}$ of up to 45 mK, sufficient to optimize both pixel types to meet our energy resolution goals. After fully fabricating and

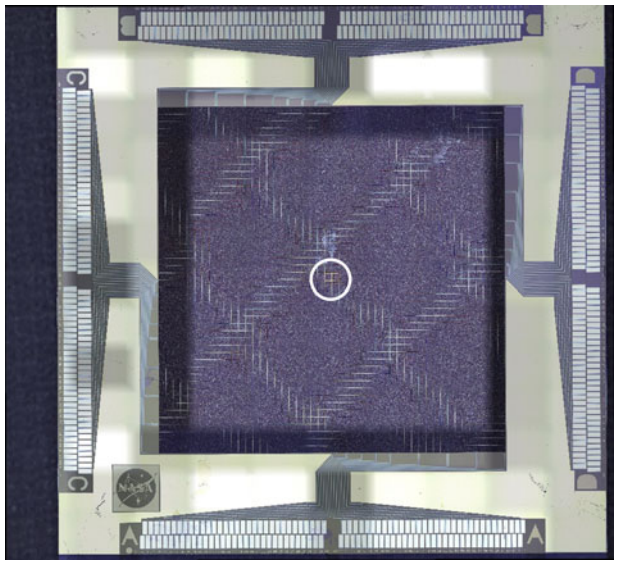

Fig. 1. We have successfully yielded a hybrid array with two distinct pixel types. The SPA (white circle) in the center region is a 10 $\times$ 10 array of 50 μm pitch pixels with a measured T_c $\sim$ 164 $\pm$ 3 mK under low $\sim$50 μA bias. The SPA rests on a single 500 $\times$ 500 μm SiN membrane. The surrounding LPA has 250 μm pitch pixels each on their own SiN membrane with a measured $T_c \sim$72 $\pm$ 2 mK.

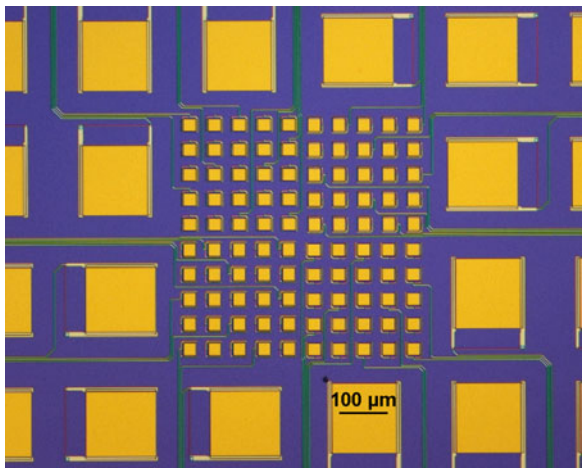

Fig. 2. Close up of the inner SPA and some surrounding LPA pixels without the cantilevered absorbers. The SPA TES is 35 μm square and the LPA TES is 140 μm square. Select pixels have been wired up with Nb leads.

yielding this hybrid array shown in Figs. 1 & 2, we wired up individual pixels for characterization. We measured T_c of these pixels by applying a triangular waveform (50 μA peak-to-peak) to the TES/SQUID circuit and observed the transition near zero bias [8]. As expected, T_c in the LPA pixels reamined close to $T_{\rm ci}$, while T_c in the SPA pixels was 60 mK above $T_{\rm ci}$, although experience tells us that the effective under-bias operating temperature T_0 of the pixel will be lower. These results are listed in Table I.

TABLE I
DETECTOR PARAMETERS

Parameter	Hybrid LPA	Hybrid SPA	Hybrid LPA	Hybrid SPA
	Fabricated		Proposed Design	
Pixel Size	247 μm	47 μm	262 μm	115.5 μm
G_b	115 pW/K	300 pW/K	115 pW/K	300 pW/K
C_V	0.80 pJ/K	0.13 pJ/K	0.80 pJ/K	0.26 pJ/K
Au	1.64 μm	4.0 μm	1.47 μm	2.03 μm
Bi	4.0 μm	0 μm	4.0 μm	4.0 μm
Mo/Au TES	50/230 nm	50/180 nm	50/210 nm	TBD
T_{ci}	75 mK	105.5 mK	95 mK	TBD
T_c [a]	72 $\pm$ 2 mK	164 $\pm$ 3 mK	90 mK	90 mK

[a] T_c was measured by applying a 15 mV sawtooth wave to the TES/SQUID bias circuit generating an excitation current of approximately 50 μA [8].

III. FABRICATION OF ABSORBERS WITH TWO DIFFERENT HEAT CAPACITIES

In order to achieve the required heat capacity and quantum efficiency in both pixel types, the composition of the absorbers must be varied. Because the Au in our two component Au/Bi absorbers consumes 80% of the total pixel heat capacity budget, while the Bi consumes only 3% [3], our strategy is to select the Au thickness that yields the desired heat capacity and then add enough bismuth to achieve the cross section necessary to meet the quantum efficiency target.

In our test devices, we started with an evaporated 20/200 nm Ti/Au seed layer over a sacrificial layer of photoresist patterned to create the stems, attachment points between the absorber and the substrate. These stems provide thermal contact to the TES and also mechanical support for the large cantilevered absorber. Through a higher temperature post-exposure bake, we reflow the resist to make a sloped sidewall for the seed layer deposition. The reflow acts consistently on all scales down to 3 μm circles used as single point attachments to the SPA pixels, though sharp interior corners have been observed to lead to nonideal photoresist sidewalls. The LPA pixels are attached to both the TES and nitride membrane through a "T" shaped stem [9].

Next, we electroplated an additional $\sim$1.5 μm uniform Au film over the entire wafer to provide protection to the sacrificial resist supporting the added metal layers. After masking the LPA pixels with a photoresist mold, we plated an additional 2.5 μm Au layer on the SPA pixels alone. Then we removed the mold resist and masked the SPA pixels in a similar fashion before plating $\sim$4 μm bismuth on the LPA pixels alone. Again, we repatterned the array for ion milling through the thick layers of plated films to separate the pixel absorbers from thermal contact with each other. Finally, we dissolved the sacrificial resist with solvents and used a critical point dry step to yield free standing cantilevered absorbers thermally anchored to the TES by a stem. Figs. 3 & 4 show the square tile pattern of absorbers left at the end of the process.

Achieving uniformity of electroplated films through a photoresist mold is challenging. Electric field crowding occurs at the edges of wide (>100 μm) microstructures and at the center

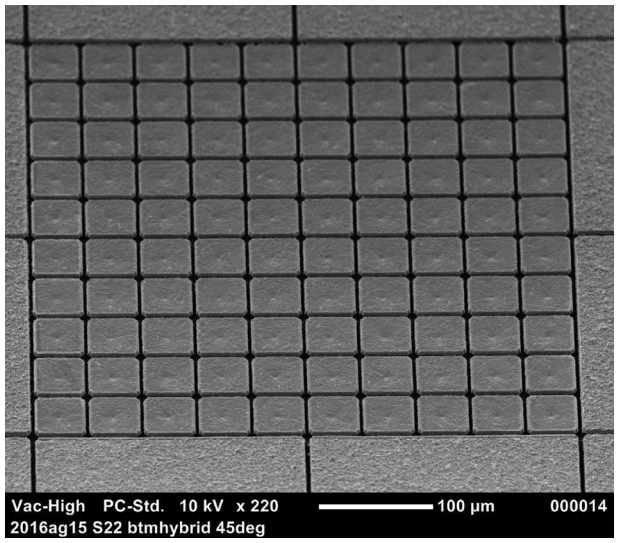

Fig. 3. SEM image at 45 degree inclination demonstrating our ability to successfully yield a hybrid array with two distinct absorber pixel types. An inner 47 μm square array of 4.0 μm thick all Au absorbers is surrounded by an outer 247 μm square array of 1.6 μm Au + 3.9 μm thick Bi absorbers pixels.

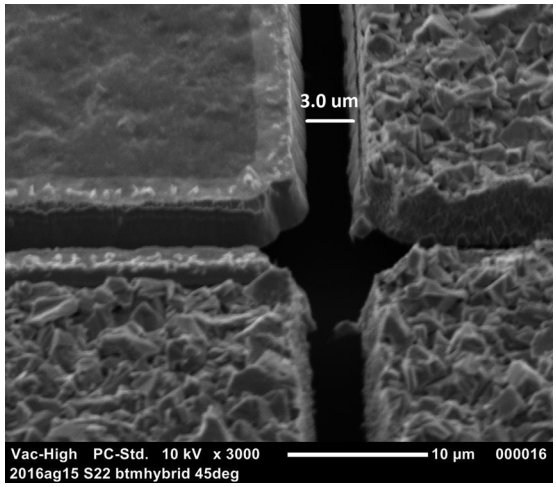

Fig. 4. We have successfully yielded a hybrid array with two distinct pixel types preserving a 3 μm gap between pixels for an 88.3% fill factor in the inner array of small pixels and 97.6% fill factor in the outer array of large pixels.

of narrow (< 10 μm) microstructures resulting in higher plating rates and thicker films in these areas (see Fig. 5) [10]. This crowding leads to "rabbit-ear" thickness profiles across large structures and rounded "cap-like" profiles across smaller structures [10]. To improve the uniformity of our electroplated films, we experimentally optimized the pulsed plating current density until we achieved the desired flat profiles across our structures. Because we observed a vertical plating thickness gradient in the bath itself, we compensated for this by a 180 degree wafer rotation at half the desired plating time.

The next challenge lay in ion milling through the thick films leaving thin streets separating pixels from thermal contact. The gaps left between pixels after milling are typically not the same as the gaps defined by photolithography. As the ion mill etches,

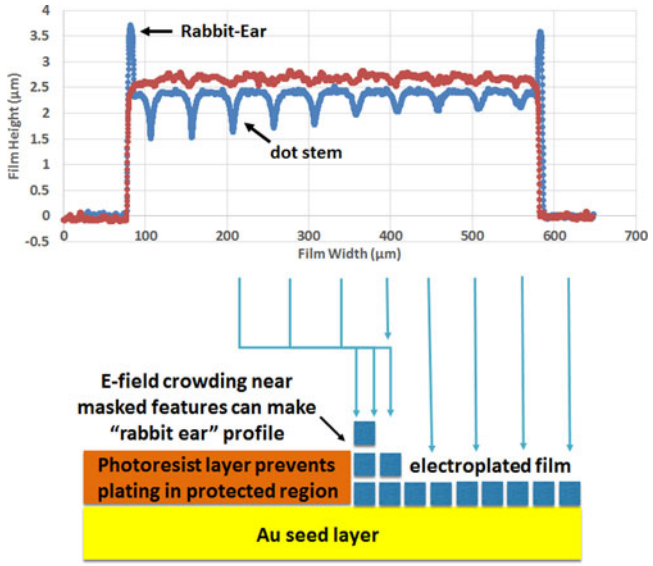

Fig. 5. The graph on top compares two step height measurements using a stylus profilometer of electroplated Au films under different bath conditions along a line crossing the 500 × 500 μm square SPA as seen in Fig 3. The dips in the lower blue profile caused by the stylus crossing the dot stems were avoided by better placement of the stylus as seen in the upper red profile. By carefully adjusting the bath conditions we were able to eliminate the "rabbit-ear" film growth and yield a uniformly thick Au layer over the area of the SPA. The bottom cartoon illustrates how E-field crowding can result in excessive film growth along the side wall of the resist mold and a rabbit-ear film thickness profile.

it sputters some of the material back onto the sidewall of the resist thus narrowing the opening for ions to penetrate the film.

We have found that for any given absorber composition there is an optimal initial photolithographically developed pattern that achieves the minimum size gap between absorbers after ion milling. Thus far, we have successfully yielded free standing absorbers in a hybrid array with ~3 μm gaps between both pixel types leading to fill factors of 88.3% for the inner SPA and 97.6% for the LPA (Fig. 3, Fig. 4).

IV. Heat Sinking for Different Pixel Types

The heat sinking requirements for the SPA and LPA are markedly different. In order to achieve the science goal of observing 10 mCrab sources at 80% throughput and <2.5 eV energy resolution, the small pixels need to be optimized for high count-rates. Until now, our small pixels have been fabricated on solid substrates with a buried copper layer to maintain a uniform heat sink temperature across all pixels and minimize thermal crosstalk [11]. By contrast, large pixels are fabricated on 0.5–1.0 μm Si_3N_4 membranes supported by a silicon framework varying in thickness between 50–100 μm depending upon the size of the TES and the maximum number of wires bundled together in a "muntin" between pixels. To minimize thermal crosstalk between pixels and increase thermal conductivity to the cold temperature bath, 3 μm thick backside copper is angle deposited along the silicon frame sidewalls but not in contact with the nitride membrane. These two fabrication techniques are incompatible for a single hybrid array.

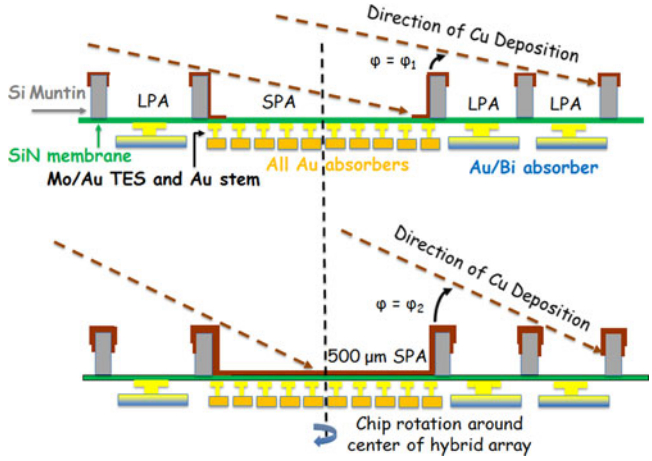

Fig. 6. Cartoon of the backside heat sinking concept for a hybrid microcalorimeter array of two pixel types (not to scale). We deposit Cu in rotation at a shallow angle (φ_1) to cover the sidewall of the SPA membrane, and then at a larger angle (φ_2) to coat the entire SPA membrane as well as the Si muntin support structure. Then we wire bond both the backside Cu and front side Au to a nearby thermal heat sink.

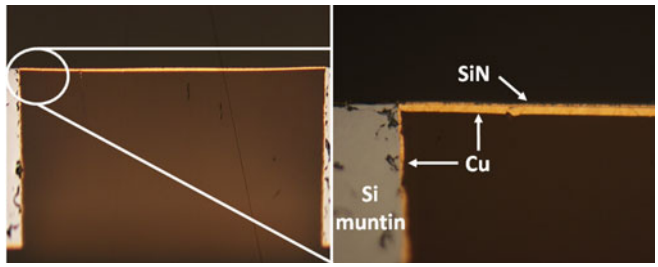

Fig. 7. Optical microscope image of a cross section demonstrating successful 3 μm Cu deposition on the 500 × 500 μm nitride membrane after deep etching through the backside of a 300 μm silicon wafer. This shows that we have the ability to thermally heat sink the entire inner small pixel array in our hybrid array design concept.

Our solution to achieving the heat sinking requirements for both types of pixels involves fabricating all pixels in the LPA on individual nitride membranes and all pixels in the SPA on a common nitride membrane and then adding copper heatsinking in a two-step backside deposition (see Fig. 6). In order to yield the membrane, we use a deep reactive ion etch (DRIE) Bosch process to remove silicon from the backside of the wafer. Because the etch rate and sidewall profiles from the DRIE depend upon geometry, one needs to optimize the recipe to yield anisotropic profiles for both types of pixels. Our fabrication procedure involved etching individual 190 μm square openings for the 250 μm pitch pixels together with a 500 μm square opening for the common central SPA. Using a protective oxide coating to protect the membrane from roughening and a low frequency pulsed plasma etch we were able to yield nearly vertical sidewalls, <2° negative profiles, for both size openings.

Next, in a two-step two-angle process we deposit copper from the backside with the goal of coating the entire sidewall and membrane of the SPA in a continuous copper sheet, while only partially coating the individual sidewalls of the muntins in the LPA. Fig. 7 is a cross section through the 500 μm wide

membrane that would support the entire SPA. One can see that we have covered the entire nitride membrane with 3 μm of copper, which forms a continuous sheet with the copper on the sidewall even at the corner where the profile of the silicon wall from the deep etch is slightly negative.

V. Flexibility of Process

The actual proposed hybrid TES array configuration differs from our experimental attempt to yield a hybrid array (see Table 1). The proposed SPA consists of 324 pixels on 115.5 μm pitch [2] and will sit atop a 2.0 $\times$ 2.0 mm square membrane, eight times larger than our successful technology demonstration of an SPA on a 0.5 $\times$ 0.5 mm square membrane. Here we discuss the risk of scaling our process to the new design proposals.

Tuning the pixels to different $T_{\rm ci}$ is done through ion milling back part of the added Au in the Mo/Au bilayer. Because our ion mill is highly uniform ($<$2% across a four inch wafer), adjusting the $T_{\rm ci}$ of the LPA by removal of Au is low risk.

The fabrication of two different absorber types involves up to three additional masks and two additional electroplating steps from our baseline uniform array process. A fourfold increase in the size of the SPA from our successful demonstration does not require any recipe changes for our electroplating through a mold procedure, because on the same test wafer and under the same current density we were able to yield uniform plating thicknesses for both window sizes. Because we are in the large microstructure regime ($>$100 μm), electroplating uniformity is not expected to present a new challenge. Further, we were able to successfully ion mill the streets leaving $\sim$3 μm gaps between pixels with different absorber compositions on 50 and 250 μm pitch simultaneously, so we do not foresee an issue yielding pixels on 115 μm pitch.

Deep etch rates and profiles vary based upon the size of the window. In a hybrid array the 2 mm $\times$ 2 mm window for the SPA is expected to etch faster and have a more negative profile than the 0.2 mm $\times$ 0.2 mm windows for individual pixels on the LPA. We will run tests to be sure we have enough silicon oxide to protect the nitride from overetch in the large SPA window until the LPA windows clear. Our two-step two-angle Cu deposition technique has been demonstrated to maintain continuity around sharp corners in negative deep etch profiles.

Uniform test arrays have demonstrated that we are able to fabricate SPA pixels on a 75 μm pitch with a 36 $\times$ 33 μm rectangular TES capable of achieving energy resolution $\sim$1eV based upon a spectrum from a 1.5 KeV Al Kα X-rays [12], and LPA pixels on a 250 μm pitch with a 140 μm square TES capable of achieving energy resolution $\sim$2 eV [9]. We will report the results of our efforts at achieving the target T_0 and energy resolution in a future publication.

VI. Conclusion

We have successfully developed and tested three separate technologies required to yield hybrid arrays with a high count-rate inner SPA as one way to meet the demanding science goal of observing a 10 mCrab source with $>$80% high resolution events. We have demonstrated the ability to tune $T_{\rm ci}$ separately for two different types of pixels. We have also yielded in a single planar process an array with different compositions of absorbers on different pixel pitch with high fill factors for maximum quantum efficiency. We have shown that we can properly heat sink both types of pixel to maintain a uniform cold bath temperature and minimize thermal cross-talk. Our process is flexible and robust, and we are in the process of fabricating and testing a complete hybrid array to measure energy resolution and other detector properties.

References

[1] X. Barcons *et al.*, "Athena: The x-ray observatory to study the hot and energetic universe," *J. Phys.: Conf. Ser.*, vol. 610, May 2015, Art. no. 012008.

[2] D. Barret, T. Lam Trong, J-W den Herder, L. Piro, X. Barcons, and the Athena team, "The athena x-ray integral field unit," *Proc. SPIE*, vol. 99052F, Aug. 2016, doi: 10.1103/PhysRevLett.104.047003.

[3] S. J. Smith *et al.*, "Transition edge sensor pixel parameter design of the microcalorimeter array for the x-ray integral field unit on Athena," *Proc. SPIE*, vol. 99052H, 2016, doi: 10.1117/12.2231749.

[4] J. E. Sadleir, S. J. Smith, S. R. Bandler, J. A. Chervenak, and J. R. Clem, "Longitudinal proximity effects in superconducting transition-edge sensors," *Phys. Rev. Lett.*, vol. 104, Jan. 2010, Art. no. 047003.

[5] J. E. Sadleir *et al.*, "Proximity effects and non-equilibrium superconductivity in trannsition-edge sensors," *Phys. Rev. B*, vol. 84, Aug. 2011, Art. no. 184502.

[6] S. J. Smith *et al.*, "Small pitch transition-edge sensors with broadband high spectral resolution for solar physics," *J. Low Temperature Phys.*, vol. 167, pp. 168–175, Feb. 2012.

[7] M. E. Eckart *et al.*, "Kilopixel x-ray microcalorimeter arrays for astrophysics: Device performance and uniformity," *J. Low Temperature Phys.*, vol. 167, pp. 732–740, Jun. 2012.

[8] K. D. Irwin and G. C. Hilton, "Cryogenic particle detection," in *Topics in Applied Physics*, C. Enss, Ed. Berlin, Germany: Springer-Verlag, 2005.

[9] W. Yoon *et al.*, "Design and performance of hybrid arrays of Mo/Au bilayer transition-edge sensors," to *IEEE Trans. Appl. Supercond.*, 2016.

[10] J. K. Luo, D. P. Chu, A. J. Flewitt, S. M. Spearing, N. A. Fleck, and W. I. Milne, "Uniformity control of Ni thin-film microstructures deposited by through-mask plating," *J. Electrochem. Soc.*, vol. 152, no. 1, pp. C36–C41, 2005.

[11] F. M. Finkbeiner *et al.*, "Development of embedded heatsinking layers for compact arrays of X-ray TES microcalorimeters," *IEEE Trans. Appl. Supercond.*, vol. 21, no. 3, pp. 223–226, Jun. 2011.

[12] S. R. Bandler *et al.*, "Advances in small pixel TES-Based x-ray microcalorimeter arrays for solar physics and astrophysics," *IEEE Trans. Appl. Supercond.*, vol. 23, no. 3, Jun. 2013, Art. no. 2100705.